LEGIBILITY NOTICE

A major purpose of the Technical Information Center is to provide the broadest dissemination possible of information contained in DOE's Research and Development Reports to business, industry, the academic community, and federal, state and local governments.

Although a small portion of this report is not reproducible, it is being made available to expedite the availability of information on the research discussed herein.

LA-UR -87-2948

3 /

CONF-8709139--1

TITLE INCREASED GAIN OF CHANNEL INTENSIFIER TUBES BY PULSED BIASING

LA-UR--87-2948

DE88 000512

AUTHOR(S) B(ruce) W. Noel, J-8
M(ichael) R. Cates, ORGDP, Oak Ridge, TN
L(arry) A. Franks, EG&G, Santa Barbara, CA

SUBMITTED TO 9th Symposium on Photoelectronic Imaging Devices,
Imperial College, London

Los Alamos

Los Alamos National Laboratory
Los Alamos, New Mexico 87545

Increased Gain of Channel Intensifier Tubes by Pulsed Biasing

B. W. Noel

Los Alamos National Laboratory, P. O. Box 1663, Los Alamos, NM 87545

M. R. Cates

Enrichment Technology Applications Center, ORGDP, P. O. Box P, Oak Ridge, TN 37831

L. A. Franks

EG&G Energy Measurements, Inc., 130 Robin Hill Road, Goleta, CA 93117

Introduction.

Although the most common use of proximity-focused channel intensifier tubes (CITs) is as optical image amplifiers, electrical gating allows them to be used as fast shutters. Except for gating, however, the effects of imposing transient or pulsed changes on CIT biases have received little attention in the literature. It would be desirable in many applications to attain the maximum possible gain, but not at the expense of reduced signal-to-noise ratio (SNR). In the experiments described here, we used pulsed biasing to increase gain; our measurements show a marked increase in gain over the dc gain without the increase in electronic noise and risk of damage that higher dc potentials create.

I. Current Flow and Gain Mechanisms.

By using a simplified analysis (Noel, Cates, and Franks, 1987), we can show that the current density at the input to the microchannel plate is

$$J = n_\phi (2e^3/m)^{1/2} |V_k + V_s|^{1/2} \ , \quad (V_k + V_s) < 0 \ . \tag{1}$$

In Eq. (1), n_ϕ is the volume density of the electrons e is the electronic charge, m is the electron mass, V_k is the photocathode bias, and V_s is the "stopping" voltage required to prevent all photocathode electrons from entering the MCP at zero bias. The absolute value of V_s, typically about 20 V (Levi, 1980), is a small fraction of V_k for normal applied bias.

For our purposes, the first stage of a CIT consists of the photocathode, the MCP input up to the first point where essentially all of the entering electrons have caused secondary emission, and the gap between the photocathode and this point. Geometrically similar to a vacuum photodiode, this stage also acts like a photodiode electrically except that the current leaving the MCP input is not identical to the photocathode current (as it would be for a photodiode anode). Instead, the current is multiplied by the first-stage secondary-emission ratio, δ_1, of the MCP material; δ_1 is a function of the primary-electron energy, eV_k.

Eberhardt (1979) has shown that MCPs behave somewhat like discrete-dynode photomultipliers of n stages, such that the electron gain is $G = \delta_1 \delta^{n-1}$, where δ is the secondary-emission ratio of each stage after the first. Under normal operation conditions, the gain relationship can be approximated by

$$\log G = k(n-1)\log(V_{mcp}/nV_c) + \log\gamma(V_k/V_c)^k \, , \tag{2}$$

which is linear in a log-log plot of G versus V_{mcp} for constant V_k. In Eq. (2), k is a constant describing the curvature of the secondary-emission function, V_{mcp} is the MCP bias, V_c is the first crossover potential (where the secondary-emission ratio is unity), and γ is the fraction of the MCP input area that will accept the electrons from the photocathode. The functional dependence of Eq. (2) holds until the MCP starts to saturate. Such saturation may be caused either by a sufficiently high current flow (space-charge buildup) to reduce the MCP's electric field significantly or by charge depletion in the walls of the microcapillaries. The "dynode" spacing is a constant given by $s = L/n$, where L is the length of the channels. Note from Eq. (2) that, if V_{mcp} is fixed, the overall gain of the $n-1$ stages following the first stage is also fixed; the first-stage gain depends on V_k.

The luminescent intensity, L, of a relatively thick layer of phosphor* is related to the accelerating

*"Relatively thick" layers are more than about 2 μm thick; such layers cause the impinging electrons to give

voltage between the MCP output and the phosphor V_{ph}, by the expression

$$L = f(i)(V_{ph} - V_0)^p , \quad (3)$$

where i is the instantaneous current striking the phosphor, V_0 is a threshold potential known as the dead voltage, and p is a number between one and two describing the exponential dependence of the particular material response. (Curie, 1963) The function $f(i)$ is linear for small currents and tends to saturate at high current densities, especially for low-energy electrons.

A. Bias and Current Limits.

The CIT requires close spacing between the photocathode and MCP input to achieve good focus. For a typical spacing of about 0.18 mm, V_k is limited to about 200 V. This value is less than the breakdown voltage of an ideal gap because of nonuniform spacing caused by irregularities in the photocathode surface. Field emission from the "high" points can give enough electrons to damage the MCP input. The phosphor requires high accelerating potential for good luminescent efficiency, so the MCP output-to-phosphor spacing is larger. typically about 1.25 mm. This spacing limits V_{ph} to about 5 kV.

Neither charge depletion nor field collapse in the MCP-to-photocathode gap due to large space-charge current is likely to cause the photocathode current to saturate in CITs. Well before either of these effects occurs, the resulting MCP output current will become excessive. Destructive current flow in the MCP can result from either excessively large photocathode current at a normal gain or excessive gain. The latter restricts the maximum dc voltage across the MCP to about 800 V. Excessive current flow can create a dead spot in the tube by destroying several adjacent micro-capillaries. In an extreme case, the entire MCP can be destroyed. Such damage may be caused by localised overheating, probably near the output end where the current density is highest. One reason we pulse the MCP (or the photocathode) to increase the system gain is that MCPs operating

---

up an appreciable fraction of their energy in the phosphor material. We used a CIT whose P-20 phosphor stratum was 25–50 μm thick.

at low duty cycles can tolerate output-current densities that would be destructive if the tubes were operating continuously at those current densities.

II. Test procedures.

In our experiments, we used an ITT type F4111 (18-mm-diam active area) with a P-20 (green) phosphor and an S-20 photocathode.

To determine the relative CIT gain, we measured the output with and without pulsed bias voltage under three operating schemes: (1) fixed V_{mcp} and V_{ph} with pulsed bias added to V_k while varying the dc level of V_k; (2) fixed V_k with pulsed bias added to the MCP dc bias while varying the dc level of V_{mcp} and V_{ph} (their sum remaining constant); and (3) fixed V_k and V_{mcp} while varying V_{ph}. Figure 1 is a schematic diagram of the CIT test configuration.

Insert Fig. 1

A short- duration ($\approx$ 9-ns full width at half-maximum) nitrogen-discharge lamp served as the light source. The pulse generator that provided primary timing for the test system served both to trigger the lamp and, through a second slaved pulse generator, to trigger a gate pulser and an oscilloscope. We adjusted the timing so that the light-output pulse occurred in the center of the gate pulse. A radiometer monitored the phosphor output.

The pulsed-bias source was a model 357A gate pulser which was designed and fabricated at the Los Alamos National Laboratory. It is an avalanche-transistor pulse generator whose pulse amplitude is -260 V and whose pulse width is determined by an attached charge line. We fixed the pulse width at 680 ns throughout the test* . In practice, the gate-pulser output was connected to either the photocathode or the MCP. In the former case, the negative-polarity pulse was square and flat-topped. When connected to the MCP, the pulse was inverted to positive by a pulse transformer. The resulting pulse had a sloping top because of the non-dc response of the inverting transformer.

*This pulse width was long enough to ensure steady-state turn-on of any sample of CIT we were likely to test. The tube we actually used turned on fully in about 10 ns.

III. Results and discussion.

A. Pulsed bias added to V_k.

The upper curve in Fig. 2 is a plot of signal amplitude versus V_k for the CIT. V_k consists of two parts: the dc bias, which was varied from -200 to +300 V, and the -260–V pulsed bias from the 357A pulser.

Insert Fig. 2

The abscissa is labeled with both the dc value, which was determined accurately, and the total value, which included an estimate of the 357A output.

For very large total negative V_k, the CIT was operating well beyond the bias limit established by the tube-component spacing and photocathode surface-uniformity estimates. In fact, with the 357A pulse added to the fixed bias, a positive dc reverse bias was required to bring the total to the calibrated value of -180 V. In this mode, the tube was gated on only during the 660 ns of the 357A pulse.

Comparing the output signal at $V_k = -180$ V and that from the highest total bias achieved, -460 V, shows a gain increase of about 50%. We observed no SNR degradation, nor was a background glow imposed over the image plane. The low duty cycle (about 5×10^{-7}) for the pulsed part of the bias provided little energy for additions to the noise characteristics established by the dc biases.

Recall that the forward section of a CIT should act like a photodiode multiplied by the first-stage gain: namely, the secondary-emission ratio, which is a function of V_k. If we divide the upper curve in Fig. 2 by δ_1, we should obtain a photodiode curve. We did this using δ *vs* accelerating potential data for SiO_2 glass (Sackinger, 1971) combined with data on δ *vs* accelerating potential at 10° grazing incidence and Hendee. (Goff and Hendee, 1967) The resulting lower curve in Fig. 2 agrees very well with the prediction.

That part of the curve to the left of -10 V total photocathode bias follows the shape predicted by Eq. (1) up to the point where the photocathode current saturates. The current density is proportional to the output signal in the test setup, provided the experiment geometry is fixed and provided the tube remains linear through its electron multiplication and electron-to-light conversion stages. Eq. (1) can be rewritten in terms of signal as $S = B|V_s + V_k|^{1/2}$, where S is the signal output and B is a proportionality constant. By fitting a square-root function through the data, we find the value of B to be about 1.8.

B. Pulsed bias added to V_{mcp}.

Because the MCP is the electron multiplier for the CIT, the dominant effect on gain by pulsed biasing should occur when one varies V_{mcp}. When we operated the MCP of our particular tube at a dc bias greater than the factory-specified nominal value of 686 V, we found a steady increase, with increasing bias, in background glow from the phosphor. It was obvious that, under these conditions, further increases in the dc bias would cause not only the SNR ratio to deteriorate quickly, but also the tube to fail. For these reasons,we limited the dc component of V_{mcp} to 775 V, which is 25 V less than the absolute maximum specified by the manufacturer.

Figure 3 summarises the features of the pulsed V_{mcp} data.

Insert Fig. 3

The lower curve shows that increased dc bias (but with no pulsed component), results in gain increases somewhat greater than a factor of ten over the practical range of MCP bias. We cannot directly compare the shape of the gain function with the expression of Eq. (2), because the value of V_{ph} decreases as V_{mcp} increases. However, the shape does show the greater-than-linear response typical of electro-optical devices with electron-multiplying stages.

The upper curve in Fig. 3 shows a significant gain increase when 260 V of pulsed bias is added to V_{mcp}. Although the dc bias was varied over a range of only 225 V, the trend of the pulsed gain increase appears consistent with that of the lower curve; i.e., an extrapolated estimate of the value of the lower curve at 810 V agrees with the actual value, on the upper curve, where the total bias is 810 V. Also, when we added the 357A pulse to V_{mcp}, the background, including the increased noise and the glow normally observed at higher dc biases, did not change measurably. Like the photocathode, then, the MCP can be operated well beyond its dc-bias range with no noise increase and no measurable device deterioration.

The upper curve reaches a limiting value of signal above a dc bias of 675 V (total bias about 935 V). Because the value of V_{ph} decreases steadily as the value of V_{mcp} increases, the saturation of the signal cannot be attributed unequivocally to MCP saturation; it could be caused by saturation of the phosphor or by space-charge limiting in the phosphor-to-MCP gap. For this reason, we explored the effects of varying V_{ph} while keeping the other biases fixed.

C. Varying V_{ph}.

The nearly linear curve in Fig. 4 is a plot of the light output when V_{ph} is varied while the total value of V_{mcp} is fixed at 950 V (686 V dc plus the 357A pulse).

Insert Fig 4

V_k was kept at -180 V, whereas we selected for V_{ph} an upper limit 10% above the tube specifications. When V_k and V_{ph} are fixed, the current at the output of the MCP is constant for constant input-light amplitude, so any increase in phosphor output signal from pulsed bias is caused by increased electron energy that results from increased V_{ph}. The figure shows that over a range of about 1.5 kV the phosphor responds nearly linearly to the increased electron energy. Thus, for V_{mcp} fixed at 950 V, there is no saturation, not even for V_{ph} as low as 3.7 kV.

Equation (3) describes the CIT's response to increased accelerating potential across the MCP-to-phosphor gap. The linearity displayed in Fig. 4 implies that the exponent, p, is approximately unity for this device, so the equation can be rewritten in terms of signal as $S = C(V_{ph} - V_0)$, where C is constant. We also assume $V_{ph} \gg V_0$ for accelerating potentials in the kilovolt range. (Curie, 1963) We then have $S \approx CV_{ph}$. For these data, $C = 200$ units/kV.

In Fig. 4, the data plotted for "varying V_{mcp}", are the data from Fig. 3 for which both V_{mcp} and V_{ph} had been varied. Like Fig. 3, Fig. 4 includes the 357A pulse as part of the total V_{mcp}. The data–now plotted as a function of phosphor voltage–still show the saturation. The crossing point of the two curves is where the tube conditions are identical for both data sets; the correspondence of all three parameters (S, V_{mcp}, V_{ph}) indicates correct normalisation.

The data below and to the right of the "varying V_{mcp}" curve display a rapid decrease in S as V_{mcp} decreases. This behavior is consistent with that predicted by Eq. (2). For this example, V_k and V_c are constant and k varies only slightly over the range of V_{mcp} encountered here, so the equation can be rewritten

$$S = D(V_{mcp})^{k(n-1)} , \tag{4}$$

where D incorporates the constant terms. Equation (4) assumes no change in V_{ph}, and there is no change for the pair of values at each position along the abscissa in Fig. 3. The only parameter difference between the abscissa values (one from the upper and one from the lower curve) is the 357A pulse present on V_{mcp} in the "with pulser" case and not in the other. We can estimate the exponential dependence of the expression by taking the ratios of several of the pairs of values, at various V_{ph} values along the abscissa of Fig. 3, to determine $k(n-1)$. We did this for values near the low-V_{ph} end of the curves where we observed no flattening in the upper curve, and found $k(n-1) \approx 9$. This ninth-power dependence of the signal on V_{mcp} completely dominates the first-power dependence on V_{ph}. This can be seen clearly in the lower-right data ($V_{mcp} < 686$ V) in the "varying V_{mcp}" curve of Fig. 4. In the upper-left portion ($V_{mcp} > 686$ V) of that curve, however, the signal limits, not increasing despite increased V_{mcp}. Our conclusion, based on the strong dominance of V_{mcp} on the signal, is that the MCP gain was limiting.

D. Further discussion and possible applications.

The use of pulsed biasing to increase the gain is limited to relatively short duty cycles. We used only one pulse width (680 ns) and a low repetition rate (10 pps). We did not try to find the point at which the duty cycle becomes excessive. We also did not have available sufficient pulse amplitude to extend the total bias to saturation (or tube failure); only the MCP appeared to saturate. Indeed, the phosphor output was linear up to the maximum available bias.

In practice, one could use pulsed bias in as many permutations as it is possible to superimpose pulses on the dc biases. For example, one could see low-duty-cycle optical transients fall within the "window" created during the pulsed bias. As another example, one could take short-duration slices out of long-duration light sources by shuttering the photocathode during the time pulsed bias is applied to the MCP and/or phosphor.

IV. Summary of study conclusions.

We added pulsed bias to both V_k and V_{mcp} of a CIT for configurations where the dc potentials on V_{mcp}, V_k, and V_{ph} were varied. Following are the main results of our experiments: (1) The photocathode responded, as predicted, like a photodiode. Inclusion of a pulsed component of V_k allowed it to be operated beyond its normal bias range. In this mode, the CIT gain increased by about 50% without SNR degradation; (2) When the MCP operated in the lower part of its bias range, its gain followed about a ninth-power dependence on V_{mcp}. The gain did saturate, but only for total biases well above the limit of dc bias that the MCP could tolerate. The pulsed-bias component on V_{mcp} added about a factor of 30 to the system gain for the nominal dc bias settings of the CIT; (3) The output signal was linearly dependent on V_{ph} for nominal values of V_{mcp} and V_k. Increasing the value of V_{ph} by 10% did not damage the tube; (4) Adding pulsed components to both V_{mcp} and V_k and operating V_{ph} 10% higher than normal can increase the CIT gain by at least a factor of 50 without significantly affecting the SNR ratio. This technique is applicable to the study of transients that are shorter in duration than the biasing pulses. CITs specially designed to exploit pulsed-biasing techniques will probably operate at even larger gain increases.

Acknowledgments.

We wish to thank John Cuny, ITT Electro-Optics Division, for participating in helpful discussions and supplying data on the CIT. We also wish to thank James D. Schoenborn for providing technical support.

References.

Curie, D. (1963). *Luminescence in Crystals,* pp. 291-292. Methuen, London.

Eberhardt, E. H. "Gain Model for Microchannel Plates," Appl. Opt. 18, 1418–1423 (1979).

Goff, R. F. and Hendee, C. F. (March 1967). "Studies of the Electron Emission Yield, Energy and Angular Distribution from High Resistance Targets at Grazing Angles of Incidence," in *27th Annual Conference on Physical Electronics,* Massachusetts Institute of Technology.

Levi, L. (1980). *Applied Optics,* Vol. 2, pp. 465–466. John Wiley and Sons, New York.

Noel, B. W., Cates, M. R., and Franks, L. A. (1987), unpublished report.

Sackinger, W. M. (1971) "Noise Performance of the Channel Electron Multiplier," in *Photoelectronic Imaging Devices,* edited by Biberman, L. M. and Nudelman, S., Vol 1, p. 181. Plenum, New York.

Figure captions.

Fig. 1. Diagram of the experiment setup used to acquire pulsed- gain data.

Fig. 2. Results of applying pulsed bias to the photocathode. Upper curve: raw data; lower curve: raw data divided by the secondary- emission ratio of the first stage of the MCP.

Fig. 3. Results of applying dc and pulsed bias to the MCP.

Fig. 4. Results of applying pulsed bias to the phosphor.

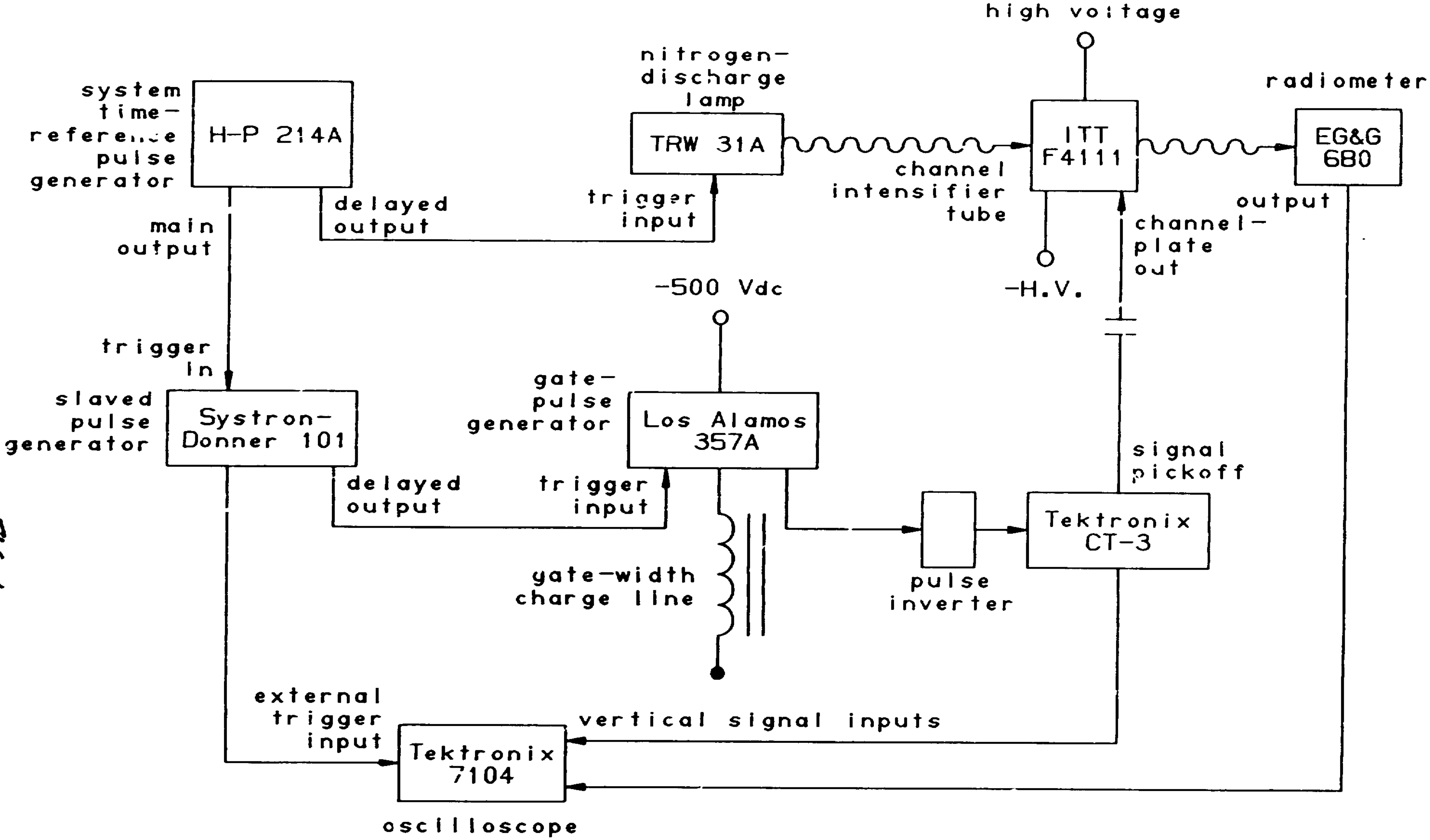
system time-reference pulse generator
H-P 214A
main output
delayed output
nitrogen-discharge lamp
TRW 31A
trigger input
high voltage
ITT F4111
channel intensifier tube
-H.V.
channel-plate out
radiometer
EG&G 680
output
-500 Vdc
trigger in
slaved pulse generator
Systron-Donner 101
delayed output
trigger input
gate-pulse generator
Los Alamos 357A
gate-width charge line
pulse inverter
signal pickoff
Tektronix CT-3
external trigger input
vertical signal inputs
Tektronix 7104
oscilloscope

FIG. 1

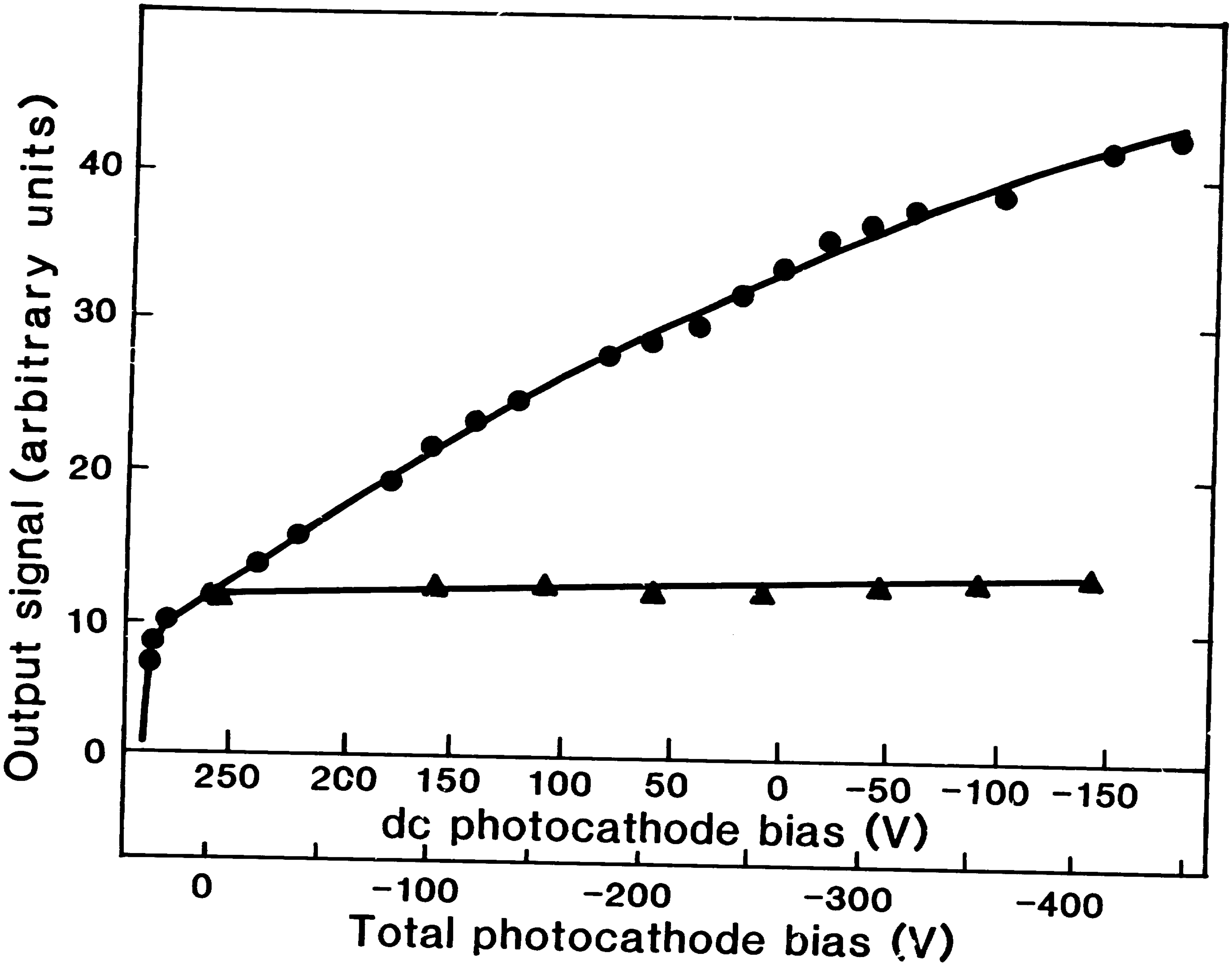
Output signal (arbitrary units)
0
10
20
30
40
250
200
150
100
50
0
−50
−100
−150
dc photocathode bias (V)
0
−100
−200
−300
−400
Total photocathode bias (V)

Fig. 2

FIG. 3

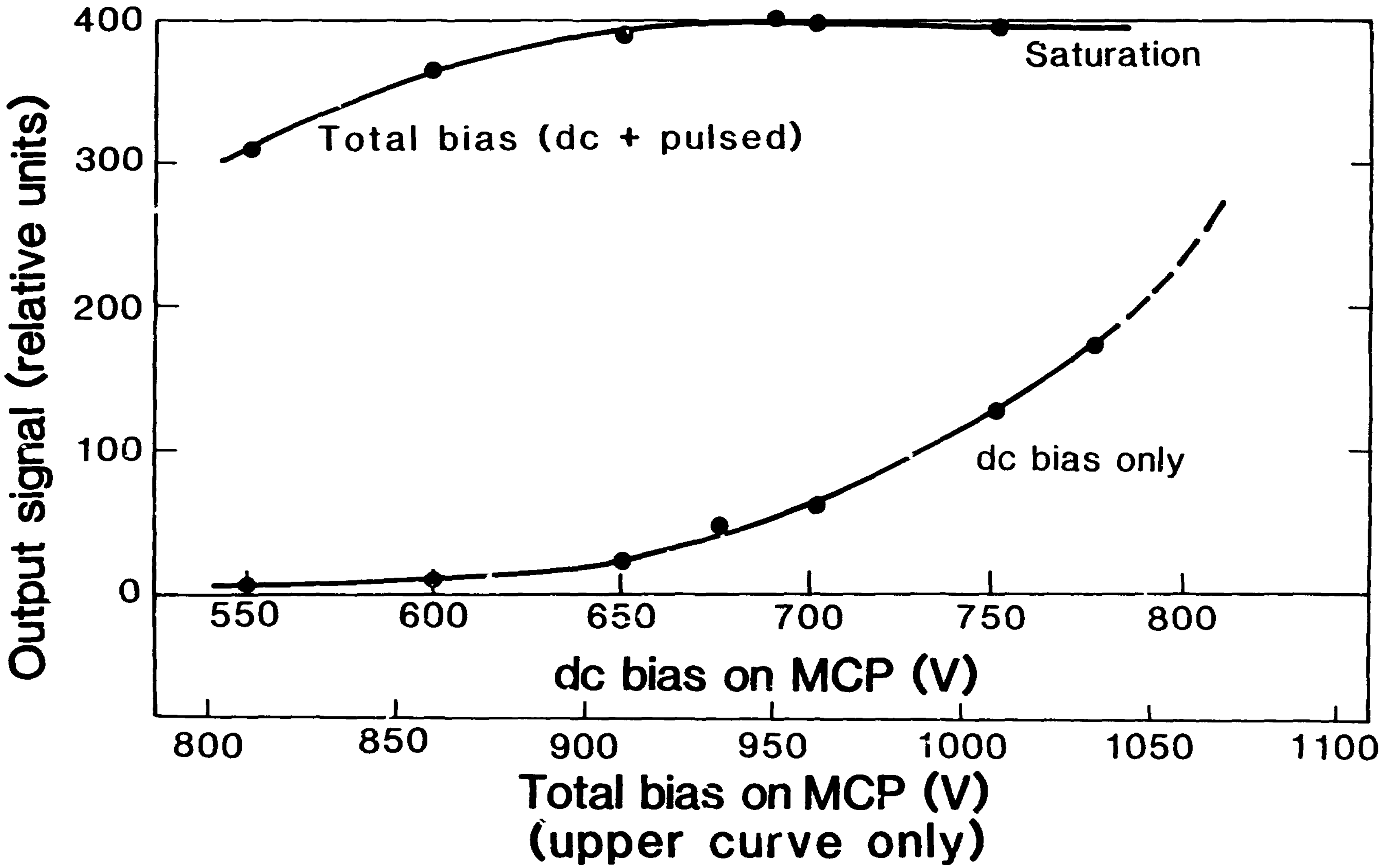
Output signal (relative units)
400
300
200
100
0
Saturation
Total bias (dc + pulsed)
dc bias only
550
600
650
700
750
800
dc bias on MCP (V)
800
850
900
950
1000
1050
1100
Total bias on MCP (V)
(upper curve only)

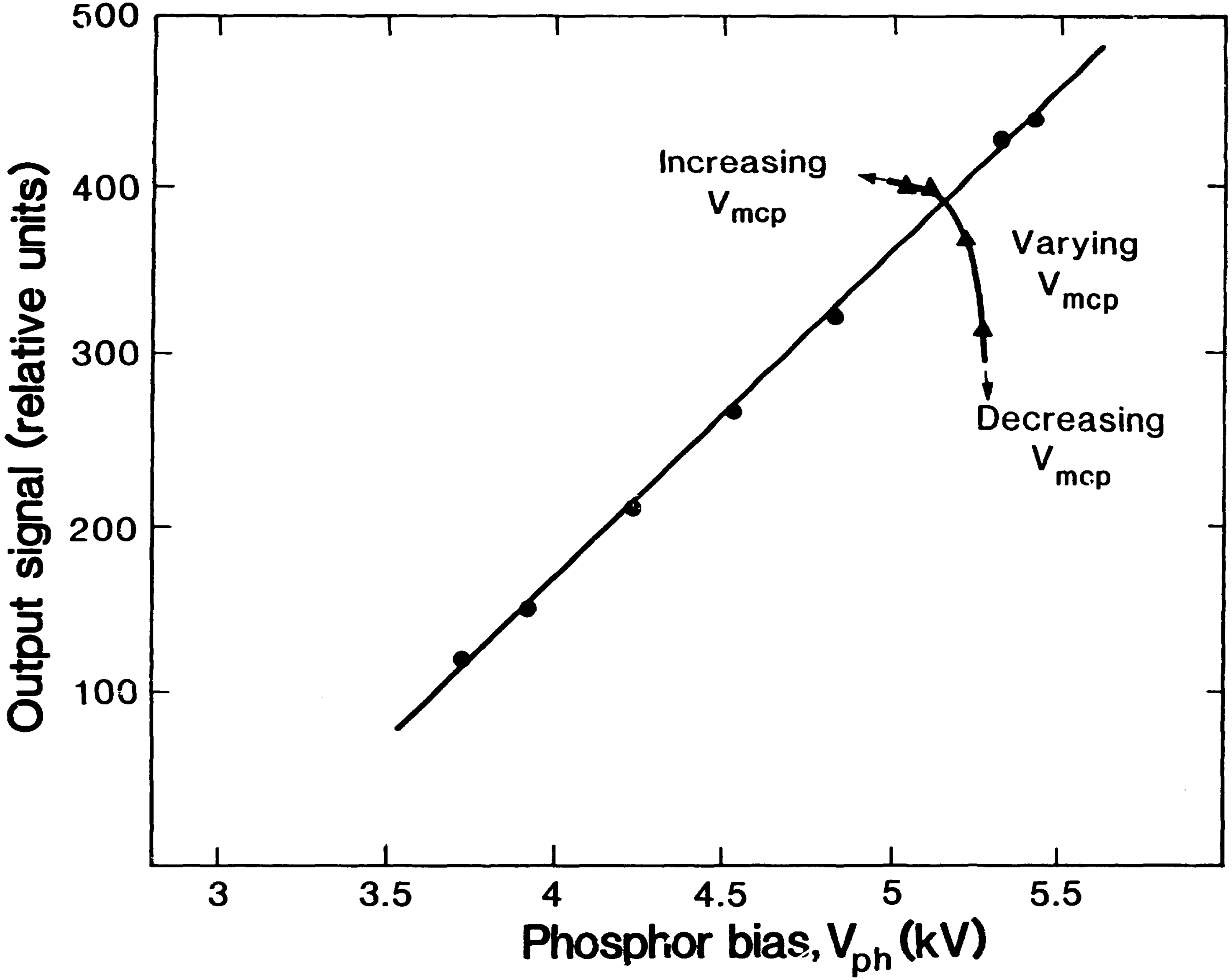

Output signal (relative units)
500
400
300
200
100
3
3.5
4
4.5
5
5.5
Phosphor bias, V_{ph} (kV)
Increasing V_{mcp}
Varying V_{mcp}
Decreasing V_{mcp}

FIG. 4